

Conditions for Jet Launching Unveiled via Multiple Ejections in XTE J1859+226

Toshihiro Kawaguchi,^{a,*} Kazutaka Yamaoka,^b Michael L. Mccollough,^c Ruben Farinelli^d and Sergei Trushkin^e

^aGraduate School of Science and Engineering, University of Toyama,
Gofuku 3190, Toyama 930-8555, Japan

^bInstitute for Space-Earth Environmental Research (ISEE), Nagoya University,
Furo-cho, Chikusa-ku, Nagoya, Aichi 464-8601, Japan

^cCenter for Astrophysics (CfA), Smithsonian Astrophysical Observatory,
B-240, 60 Garden St., Cambridge, MA 02138, USA

^dINAF – Osservatorio di Astrofisica e Scienza dello Spazio di Bologna,
Via P. Gobetti 101, I-40129 Bologna, Italy

^eSpecial Astrophysical Observatory of the Russian Academy of Sciences,
Nizhnij Arkhyz, 369167 Karachayevo-Cherkessia, Russia

E-mail: kawaguti@eng.u-toyama.ac.jp, yamaoka@isee.nagoya-u.ac.jp

We investigated the X-ray, soft gamma-ray and radio data of the Galactic black hole binary XTE J1859+226 in the 1999–2000 outburst. This object showed 5–6 discrete jet ejections within about 30 days around the peak of the outburst, and thus is suitable to figure out what are the precursors of radio flares and what drives the discrete jet ejections. We found that jet ejection events occur when the inner radius of the accretion disk (R_{in}) rapidly approaches the innermost stable circular orbit (ISCO). Namely, the time derivative of R_{in} is likely the key parameter to launch jets. Given the correlations among the X-ray fractional variability amplitude (rms), R_{in} and the X-ray hardness, previous phenomenological arguments related to jet ejections ("jet line" and sharp drops of rms) seem to be physically caused by the time variation of R_{in} . (I) A rapid shrinkage of R_{in} down to the ISCO can be a useful index for triggering Target-of-Opportunity observations to catch the moment of the discrete jet production. (II) When R_{in} is already at the ISCO, jet ejections are not expected for a while until it leaves the ISCO and gets ready for the next shrinkage of R_{in} . (III) It would provide constraints on jet launching mechanisms. A model which launches jets all the time when R_{in} is at the ISCO would have difficulties. We also show how these conditions work in other objects, and discuss towards the "jet forecast".

87th Fujihara Seminar: The 50th Anniversary Workshop of the Disk Instability Model in Compact Binary Stars (DIM50TH2025)
22-26 September 2025
Tomakomai, Japan

*Speaker

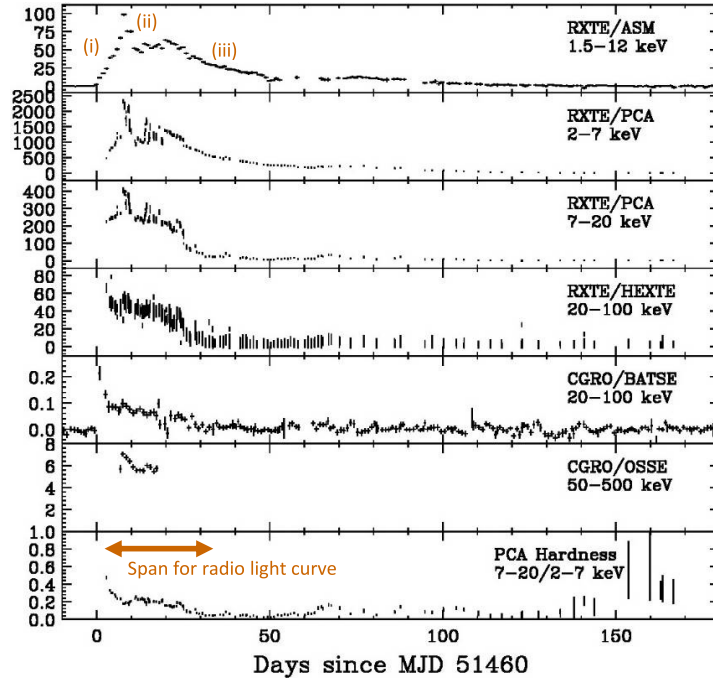


Figure 1: Light curves in X-ray and soft Gamma-ray, as well as the time evolution of the X-ray hardness. Horizontal arrows in the bottom panel show the time span over which the radio light curve is shown in figure 2. Original figures are presented in [1].

1. XTE J1859+226

Relativistic jet ejections are universally formed by black holes (BHs) from stellar to super-massive masses. Although more than a century has passed, its launching mechanisms are still unclear. We then searched for conditions (or precursors) of such discrete jet events, by focusing on an X-ray binary system, XTE J1859+226 [1]. As we will see in the next section, this object has shown several, discrete jet ejections on a short timescale, and thus is suitable for investigating the jet physics.

This binary, with a $\sim 8M_{\odot}$ BH [2], was found about 25 years ago with the RXTE satellite, by a half-year outburst as shown in figure 1. For the first ~ 30 days, the radio light curve is also shown in figure 2. Jet ejections during this outburst, around the peak X-ray brightness, is the main topic of this article.

After a brief summary of the outburst event and jet ejections, we show the combined analysis using the X-ray and radio data in the next section. Then, we tried to figure out what is going on ahead of each discrete jet ejection in the subsequent section. Results obtained for other binaries are followed.

2. Time evolution during the outburst in 1999

Here, we describe the outburst event in more detail. Figure 1 shows several light curves in X-ray and soft Gamma-ray (1.5–500 keV) over the half year (through ASCA, BeppoSAX, RXTE,

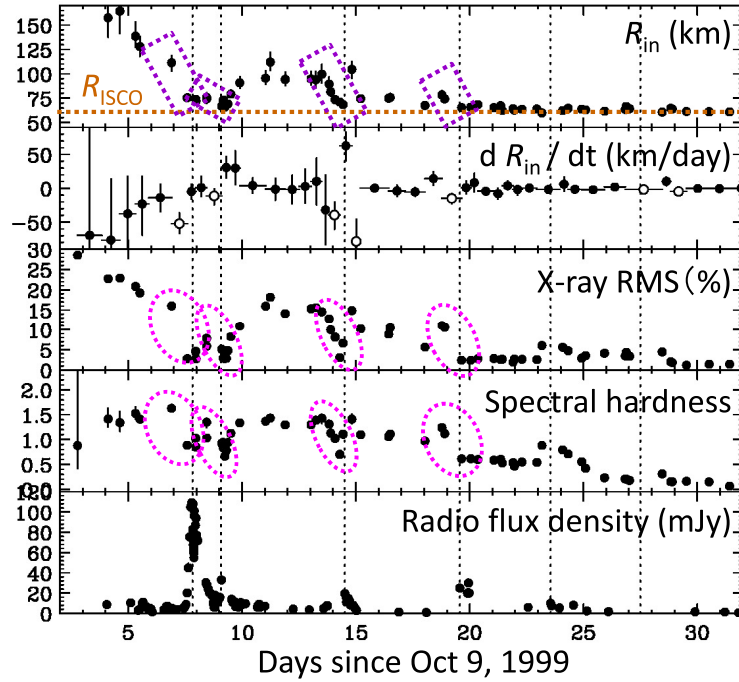


Figure 2: Time variation, over the 30 days relevant to the jet ejections, of the inner radius, its time derivative, the X-ray variability amplitude rms, the X-ray spectral hardness (between the Comptonized flux and the disk direct flux), and the radio flux density [1]. Horizontal dashed line in the top panel indicates the putative ISCO radius, while vertical dotted lines indicate the timing of jet ejections.

and CGRO), as well as the time evolution of the X-ray hardness. The conventional X-ray hardness v.s. intensity diagram during these observations is shown in figure 3 (upper panel). In terms of the state transitions, this source moved from the hard state to the soft state, and then all the way back to the hard state again. Namely, this object is quite usual in this sense.

A spectacular point of this source is that several, discrete jet ejections, within ~ 30 days around the peak of the X-ray brightness, were reported [1, 3]. Timing of jet ejections are shown by vertical dotted lines in figure 2. In other words, this source is very useful for investigating which quantity shows a characteristic behavior before jet ejections, and then which physical condition is necessary for launching discrete jets.

Here, we shortly mention the spectral and timing properties that we used. More details are described in [1]. The X-ray spectral analysis in our work is quite conventional. We have a multi-temperature accretion disk, from which we deduce the temperature of the inner disk, T_{in} , and the inner radius, R_{in} . We mainly focus on the inner radius in this article. We also have a Comptonized, power-law component, which consumes a part of the disk photons. This component represents a hot (i.e., radiatively inefficient) plasma, such as the corona above and below the disk or an advection-dominated accretion flow (ADAF). Another ingredient in our analysis is the X-ray, fractional variability amplitude, rms [4]. Figure 2 shows the time evolution of R_{in} , rms, the X-ray hardness, and the radio flux density.

The lower panel of figure 3 shows the time evolution of R_{in} and the disk flux. Different colors

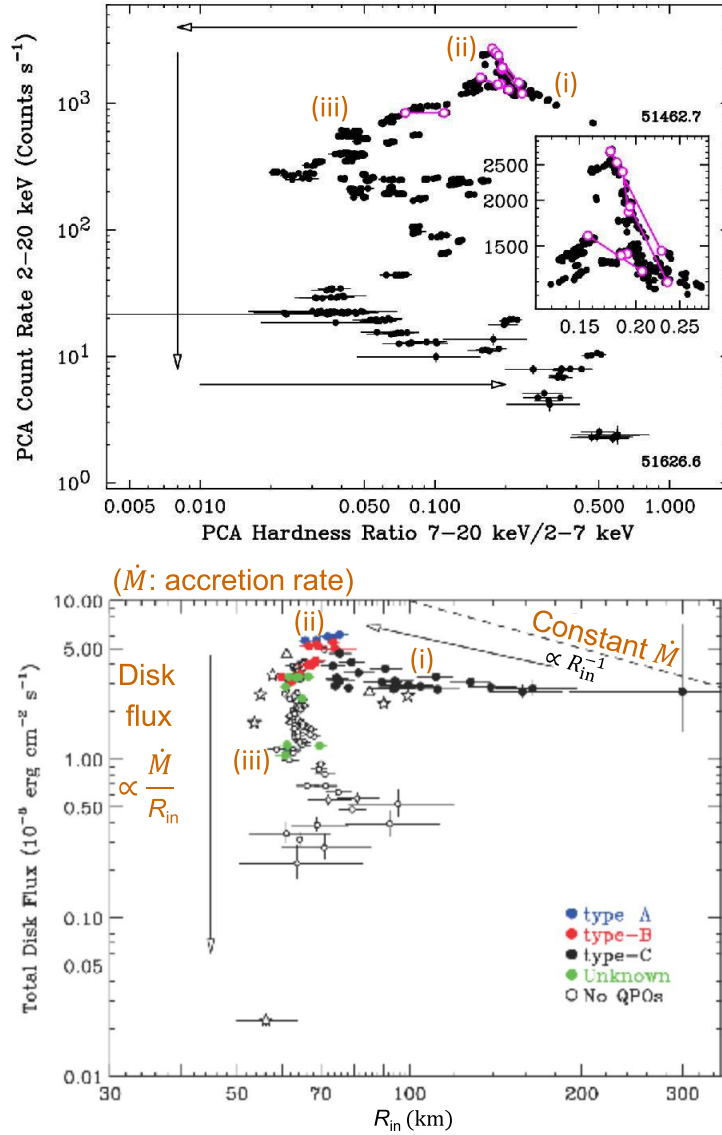


Figure 3: Conventional diagram describing the X-ray hardness and the intensity (upper panel). The inset is a close-up view around the jet ejections. For each jet ejection, two epochs just before and after the jet production are shown by open circles and connected by a solid line. The disk flux-to-inner radius diagram (lower panel) [1], by which we can estimate the time evolution of the accretion rate during the outburst.

of the data points indicate different QPO types. Discussions on various quantities as a function of QPO types, the possible configuration relevant for each QPO type, and the origin for QPO types are presented in [1]. For instance, by plotting the QPO frequencies as a function of R_{in} , we argue that the Lense-Thirring precession has a difficulty in explaining the QPOs. In this article, we concentrate ourselves on the jet conditions, and skip the QPO issues.

The time evolution of the temperature of the inner disk, rms, and the X-ray hardness are shown in figure 4. At the beginning of the observations [hereafter, stage (i)], the disk was far away from the BH (figures 3, 4). Then, it approaches the black hole, increasing the inner disk temperature.

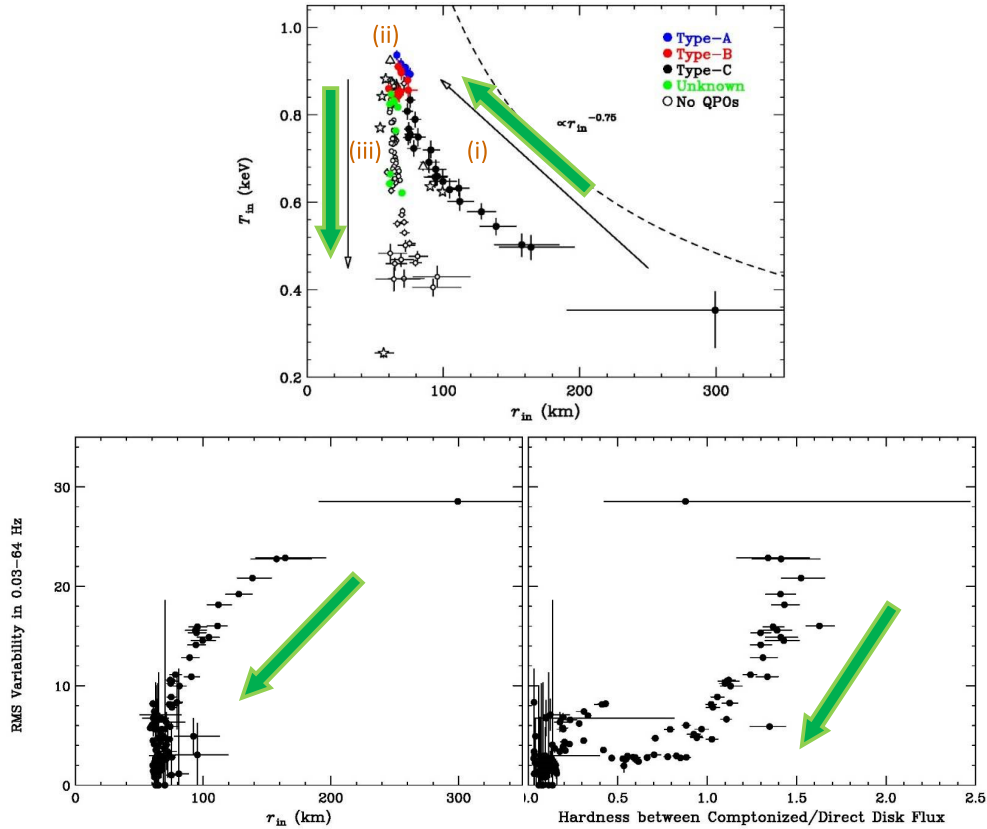


Figure 4: Correlation we found among the inner radius R_{in} , the variability amplitude rms and the spectral hardness of the X-ray components [1]. Arrows indicate the time evolution during the outburst.

After reaching the maximum temperature and the peak X-ray flux density [stage (ii)], the disk is getting cooler [stage (iii)].

The bottom two panels of figure 4 show the correlation we found among the inner radius R_{in} , the variability amplitude rms and the spectral hardness of the X-ray components. As the inner radius gets smaller, we see less X-ray variability and softer X-ray spectra. It means that the X-ray variability is controlled by the competition between the relatively stable disk and the highly-variable hard component.

Then, we estimate the accretion rate, \dot{M} , during the outburst. Figure 3 presents the X-ray, hardness-to-intensity and the disk flux-to-inner radius diagrams. Given that the disk flux is likely proportional to \dot{M}/R_{in} , we can infer the accretion rate from this disk flux-to- R_{in} diagram. If the accretion rate is fixed at a certain level, then an object is supposed to move along the inclined, dashed line ($\propto R_{\text{in}}^{-1}$).

In the first 10 days [stage (i)], the X-ray flux density increases very quickly (figure 1). However, the accretion rate seems to *decrease* in this brightening phase (figure 3). The accretion rate has the maximum value at the beginning and becomes smaller by a factor of ~ 3 . Because of the shrinkage of the inner radius, the disk flux itself becomes larger towards the peak of the X-ray brightness. The large accretion rate at the beginning is also supported from the hardness-intensity diagram

(upper panel). The time evolution of the outburst starts from the upper-right corner, rather than the conventional lower-right position.

After the X-ray peak brightness [stage (ii)], the source is getting dimmer over ~ 5 months [stage (iii)], reducing the accretion rate further by a factor of ~ 3 hundreds. Then, this object returns back to the hard state again.

In this article, we focus on the multiple jet ejections [in the stage (ii)] around the epoch of the X-ray peak flux density, which corresponds to about 60% of the Eddington luminosity. During these jet ejections, there is no obvious jump or sudden increase of the accretion rate (lower panel of figure 3). In other words, something else, other than the accretion rate, must control the jet production.

3. Precursors ahead of each jet ejection

Figure 2 shows a closer view of the 30 days relevant to the jet ejections. In the top panel, we see the inner radius R_{in} stays at ~ 64 km, which is likely the putative innermost stable circular orbit (ISCO), in the latter half (after ~ 20 days). We also present the X-ray variability amplitude, the X-ray spectral hardness and the radio flux density. Vertical dashed lines indicate the timing of the discrete jets, estimated from radio observations.

Before describing our analysis, we briefly touch on the two, conventional arguments on the timing of jet ejections. Firstly, a jet is launched when a source crosses the “jet line” (between the hard and the soft states) leftward in the hardness-intensity diagram [5]. In terms of the time series in figure 2, we do see the drop of the X-ray hardness at the jet timing. However, it is not straightforward to forecast a jet production based on the X-ray spectral hardness. In the upper panel of figure 3, these jet ejections are indicated by connecting the two data-points, just before and after the jet ejections. There is no single line, over which all the jet events pass. Moreover, there are many epochs near the pairs showing jet ejections, but most of them do not pass leftward by the next exposure. Therefore, from the position in the hardness-intensity diagram, we can *not* predict the timing of the coming jet.

Next argument of the jet timing is the X-ray variability amplitude rms. For several objects, sharp drops of the variability amplitude are associated with radio activity within a few days [6]. Again in the time series (figure 2), we see the drops of rms before jet ejections. However, it is not clear yet to what extent the variability amplitude must be reduced for launching jets. Moreover, plausible physics behind the connection between rms and jet ejections are also unclear.

When we saw the time series for a variety of quantities as shown in figure 2, we realized that a rapid shrinkage of the inner radius and arrival of R_{in} at the minimum value happen just ahead of each jet ejection. We then came to the idea that a discrete jet can be launched when the following two conditions are satisfied. First, the inner radius shrinks sufficiently fast, and secondary, it reaches the ISCO.

The second panel of figure 2 shows the time derivative of the inner radius R_{in} . The open symbols mean that the time derivatives (\pm error-bars) of R_{in} at those epochs are definitely negative. Overall, the negative time derivatives seem to happen ahead of each jet ejection. It indicates that discrete jets are launched when R_{in} shrinks down to the ISCO fast enough. Then, we wanted to investigate this scenario in a quantitative way, analyzing the radio light curve more.

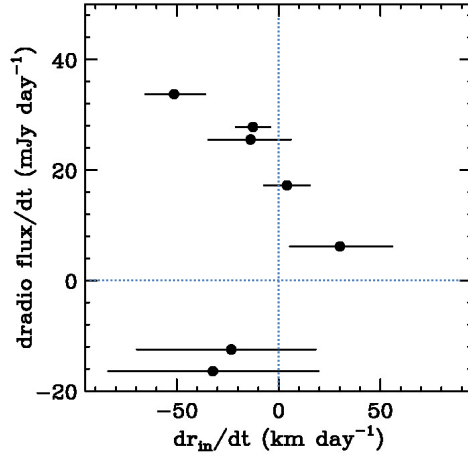


Figure 5: The slope in the radio light curve as a function of the time derivatives of R_{in} .

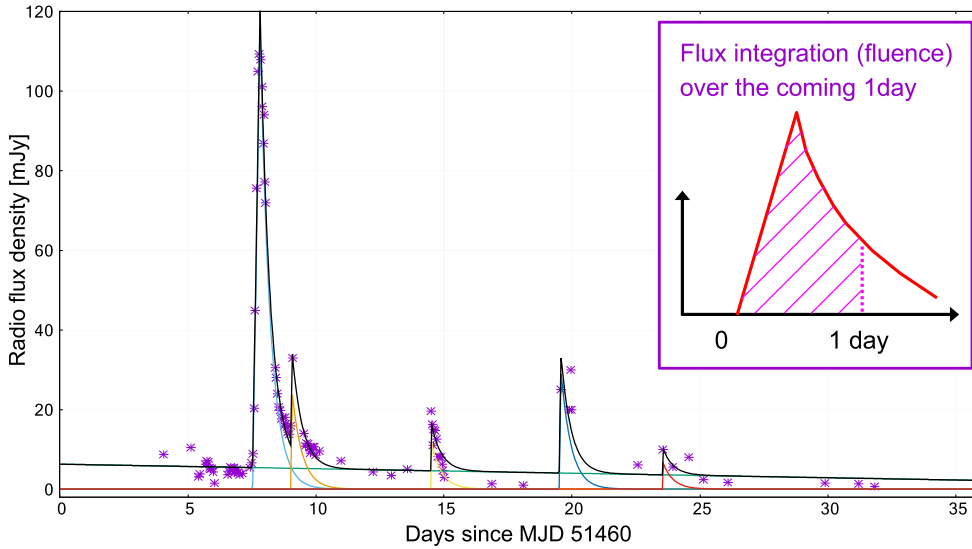


Figure 6: Our fitting result for the radio data, comprising a linear component (nearly horizontal, straight line) and five FRED-type flares (five, FRED-shaped lines). Then, the radio activity within the coming one-day is calculated to investigate the relation with the time variation of X-ray data (figure 7).

Figure 5 shows our first trial, comparing the time derivative of the inner radius and the slope of the radio light curve within a certain time-interval from the X-ray measurement. For a time/epoch when the time derivative of X-ray spectral fitting (e.g., R_{in}) is available, if more than two radio measurements are recorded within the coming 0.3 day, we calculate the slope of the radio light curve within the 0.3-day interval via the least square fit. When we made this plot, we had a positive impression, because the rapid shrinkage of the disk inner radius tends to show the radio brightening thereafter. This encouraged us towards further radio analysis to measure the jet power more directly.

Then, we try to fit the radio light curve. The radio time variation by a jet production, shows a fast linear rising, followed by an exponential decay (FRED) [7]. Figure 6 is our fitting result for the

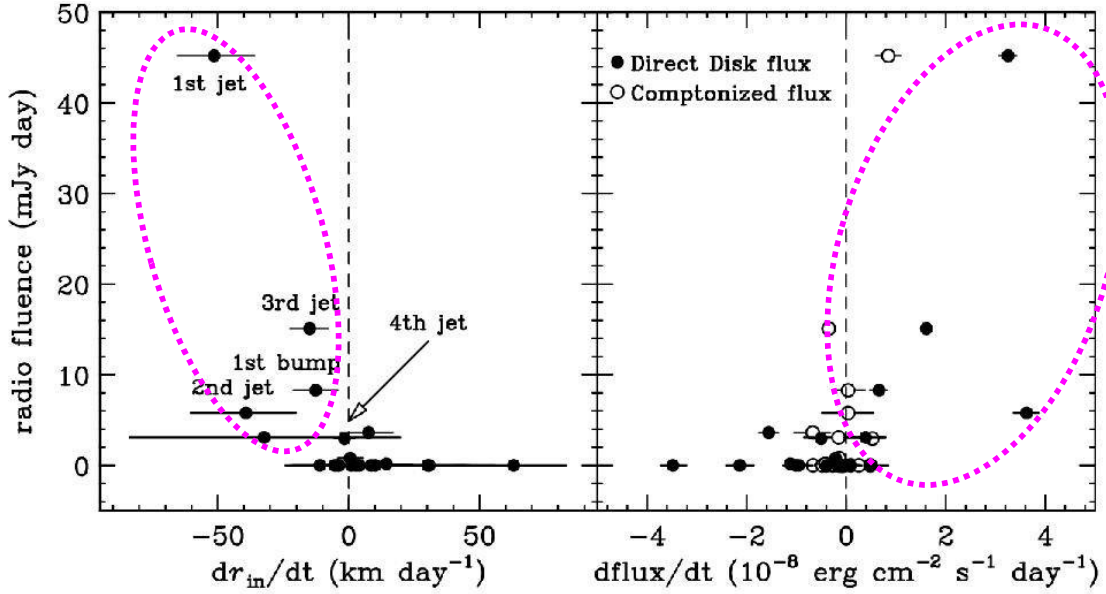


Figure 7: Radio fluence within an one-day interval, the power of the coming jet, as a function of the time derivative of the disk inner radius (left). Time derivatives of the disk and the Comptonized fluxes are also compared with the radio activity (right) [1]. Ellipses indicate the trend of (anti-)correlation, and are drawn to guide the eye.

radio data. It is a combination of a linear component plus five, FRED-type radio flares, for which we assumed a common rising rate. By fitting the light curve, a typical timescale of a radio flare (the rising plus the decaying e-folding timescales) for this object is found to be about 1 day. A log-scale version of the radio fitting is shown in [1], where an additional radio flare, between the first two jet ejections reported in [3], is visible more clearly.

After fitting the radio light curve, we then integrate the fitted flare over the coming one-day interval from the epoch of each X-ray measurement. In other words, the flux integration, fluence, is measuring the power of the next, upcoming jet.

Figure 7 shows the radio fluence, the jet power, as a function of the time derivative of the disk inner radius. Again, we see a trend of anti-correlation between the two quantities. In other words, when the disk inner radius rapidly shrinks (leading the increase of the disk flux), then a jet is launched within the coming one day. On the other hand, we see almost no jet ejections when the time derivative is positive or zero. We now propose that the time derivative of the disk inner radius is the key parameter to launch discrete jets.

In the right panel, we also compare the power of the jet ejections with the time derivative of the fluxes of either the disk or the hard, Comptonized components. Associated with each radio flare, the disk becomes bright because of the shrinkage of the inner radius. In contrast, little time variation of the Comptonized component happens ahead of jet ejections. If a part of the corona or the ADAF is the origin of the jets, we would expect a considerable time variation of the coronal or the ADAF emission before jet ejections. However, it turned out that it is not the case. Thus, the jet material may come from the disk, rather than the corona or the ADAF.

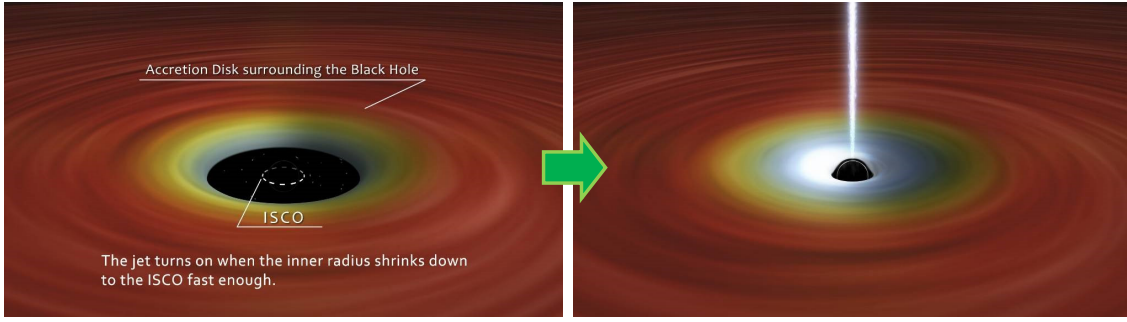


Figure 8: Cartoon for time evolution of the system. We propose that discrete jets are launched when the disk inner radius shrinks down to the ISCO fast enough.

Figure 8 presents a cartoon of the time evolution of the system¹. At the beginning, the inner radius was far away from the ISCO. Then, the jet is launched when the disk shrinks down to the ISCO fast enough. The inner radius then increases, and gets ready for a next shrinkage. On the other hand, when the inner radius stays at the ISCO, a new jet ejection is not expected. Then, one can remain unfazed and has time for arranging observational facilities waiting for the departure of R_{in} from the ISCO. Theoretical models for launching relativistic jets will need to work in a dynamic condition.

4. How it works in other objects: Towards the "jet forecast"

As a next step, we need an investigation to make sure that the same or similar conditions do work in other objects. If it is the case, it is quite practical and productive procedure. Monitoring of the inner radius, by a sort of pipe-line products, to predict the timing of jet production, will raise the success rate of Target-of-Opportunity (ToO) observations. Namely, the (approved) observing time can be used selectively in the expected timing of jet productions. Then, better quality-data with more frequent cadence will be obtained in the future, from which we will see how fast dR_{in}/dt must be for launching a discrete jet. This kind of "jet forecast" would accelerate the understanding of jet physics.

We have seen that the association between jet ejections and the X-ray variability rms was found for multiple objects [6] and that there is a beautiful correlation between the variability and the disk inner radius for XTE J1859+226 (figure 4). Then, we expected to obtain a similar behavior (i.e., rapid shrinkage of the disk inner radius) ahead of a radio activity, and to see a correlation between R_{in} and rms in other binaries.

We did analyses of similar sources (XTE J1550–564 and GX 339–4). For XTE J1550–564, we show the time evolution of various quantities in the left panel of figure 9. In this 100-day time series, there is a radio flare (bottom panel). Ahead of the radio activity, there are a drop of the X-ray variability (second panel), and a rapid shrinkage of the disk inner radius (top panel). In the right panel, we see that filled circles, XTE J1550, show a relation between the inner radius and

¹Movie files are available at homepages of TK (<http://www3.u-toyama.ac.jp/kawaguti/researchE.html>) and KY (<https://www.isee.nagoya-u.ac.jp/en/news/research-results/2025/20250507.html>).

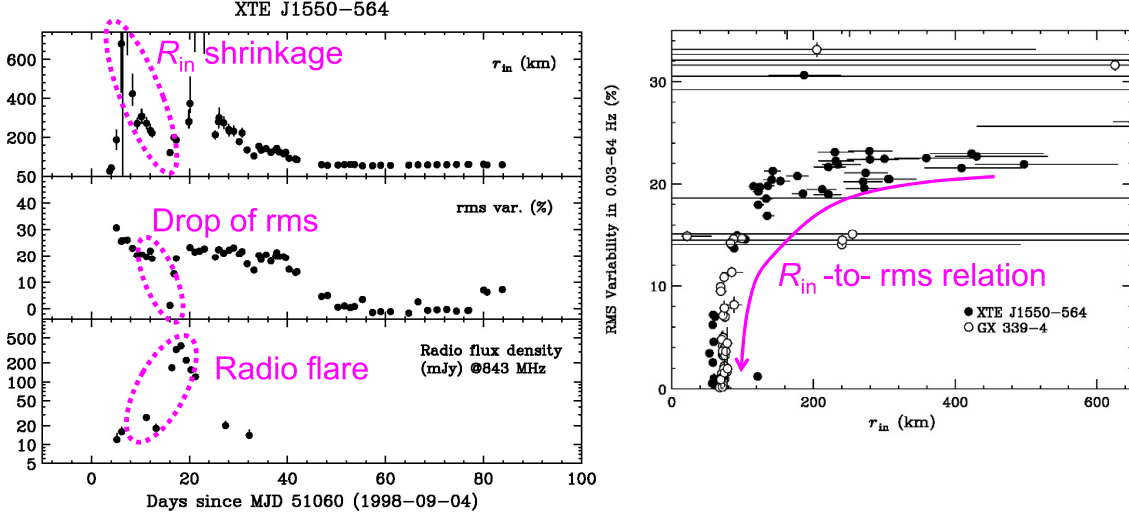


Figure 9: Time variation of various quantities over 100 days of XTE J1550-564 (left). Relation between R_{in} and rms (right) for XTE J1550-564 (filled circles) and GX 339-4 (open circles).

the X-ray variability amplitude. Namely, this is another example that shows both a precursor of a discrete jet ejection and the correlation between R_{in} and rms. This is an encouraging finding towards establishing the "jet forecast". More details will be presented elsewhere.

Here, we emphasize the advantage of the time derivative of the inner radius. We are arguing that monitoring the inner radius, to search for a rapid shrinkage down to the ISCO, is a useful index for starting ToO observations to catch the jet production event. This procedure is quite effective for sources with known ISCO radii, which we estimate from the time series of the radius (figure 2), or the inner radius at the epoch of a jet ejection. Compared with this dR_{in}/dt procedure, the two conventional arguments on the jet timing have difficulties in predicting when a next jet is launched. In the hardness-intensity diagram, there are many epochs near the jet line that do not show radio activities by the next exposure. In terms of the X-ray variability amplitude, rms, we do not know the threshold of rms to launch jets. On the other hand, we have a reference point for the inner radius R_{in} (figure 2), which is probably the ISCO.

Moreover, we note a characteristic shape in the rms- R_{in} diagrams (lower-left panel of figure 4 and right panel of figure 9). Namely, both objects (XTE J1859+226 and XTE J1550-564, respectively) show a convex-upward form in the diagrams. For the former, we found a relation as $rms[\%] = 33.0 - 25.3(R_{in}/70[km])^{-1.01}$ [1]. For the latter (figure 9), the convex is even stronger. This convex-upward shape means that the shrinkage of R_{in} does not associate a sharp drop of rms in the beginning. In other words, the rapid decrease of R_{in} starts earlier than that of rms. Later, the R_{in} -shrinkage and the drop of rms together keep step to a jet production. In terms of the "jet forecast", the monitoring of R_{in} is thus a more effective tool to notice (and start a careful watch on) a coming jet ejection, than that of rms. The convex-upward shape also means that various rms values appear when R_{in} stays around the minimum radius (figures 4 and 9). It can be a reason why it is still unclear to what extent rms must be low for a jet ejection.

In XTE J1859+226, the shrinkage of R_{in} seems to start about 1-2 days before the onset of the

rising in radio flux density (figure 2). While, in XTE J1550–564, it seems to start about 5–10 days before a radio flare (left panel of figure 9). Better-quality data, which will be obtained via the "jet forecast", would uncover what determines these timescales.

When both the R_{in} -shrinkage and the rms-drop happen, alerts can be sent and then ToO observations will be worthwhile to be performed. For XTE J1859+226, for example, a half-day can be spent for discussing whether they start a ToO observation or not. If the rapid, decreasing trend of both R_{in} and rms (as well as the spectral hardness) continues during the half day and if R_{in} almost reaches the ISCO, then an observation can be started after a preparation in a few hours. For XTE J1550–564, we will have more time to make a decision and to prepare ToO observations.

5. Summary

To investigate what drives the production of discrete jets from the vicinity of BHs, we searched for conditions (or precursors) of such jet events.

Firstly, we took a close look at the X-ray and radio data obtained for a binary system, XTE J1859+226 [1]. By calculating the time derivatives and integrals of the data and various quantities, we eventually found the conditions for the jet launching events. We argue that a rapid shrinkage of the disk inner radius down to the ISCO is the condition for jet production. We also found strong correlations among the X-ray variability, the inner radius, and the X-ray hardness. Therefore, two phenomenological arguments so far on jet productions, "jet line" and drops of the X-ray variability amplitude, seem to be physically caused by the time derivative of the disk inner radius. We think that the monitoring of the inner radius has more predicting power for the jet timing, because there is a reference point in the radius, which is likely the ISCO.

Next, we examined additional objects to see whether the same or similar condition works other than XTE J1859+226, and found that XTE J1550–564 does show the similar behavior in the timing and spectral properties. It is necessary to confirm that it is the case for many binaries as well (beyond a couple of objects shown in this article). If it turns out to be true, there are several perspectives.

- (I) By monitoring the inner radius to predict the timing of jet ejection, we will have more successful ToO observations. Thus, this "jet forecast" will be a practical and productive procedure to obtain a good-quality data.
- (II) When the inner radius is at the ISCO, jet ejections are not expected for a while, until it leaves the ISCO and gets ready for the next shrinkage. It means more time to arrange for additional satellites/observatories aiming at observing the next, upcoming jet ejection.
- (III) For theoretical aspects, models that eject jets in a static condition, for instance all the time when the inner radius is at the ISCO, would need to be modified. Models that work in dynamic condition(s) are favored. To be precise, this conclusion itself is not a new finding. The same conclusion comes from no jet ejection in the soft state.

Acknowledgments

We are grateful to Christian Knigge and Chris Done for helpful comments on the presentation during the workshop. TK acknowledges the support by the Thirty Meter Telescope (TMT)

Project, National Astronomical Observatory of Japan, through its funding program for research and development of TMT science instruments, and by JSPS KAKENHI Grant Number 25K07370.

References

- [1] K. Yamaoka, T. Kawaguchi, M.L. McCollough, R. Farinelli and S. Trushkin, *X-ray Spectral and Timing Properties of the Black Hole Binary XTE J1859+226 and their Relation to Jets*, *PASJ* **77** (2025) 237–259.
- [2] I. V. Yanes-Rizo, et al., *A refined dynamical mass for the black hole in the X-ray transient XTE J1859+226*, *MNRAS* **517** (2022) 1476.
- [3] C. Brocksopp, et al., *Initial low/hard state, multiple jet ejections and X-ray/radio correlations during the outburst of XTE J1859+226*, *MNRAS* **331** (2002) 765.
- [4] P. Casella, T. Belloni, J. Homan, & L. Stella, *A study of the low-frequency quasi-periodic oscillations in the X-ray light curves of the black hole candidate XTE J1859+226*, *A&A* **426** (2004) 587.
- [5] T. Belloni, *States and Transitions in Black Hole Binaries*, *LNP* **794** (2010) 53.
- [6] R. P. Fender, J. Homan, & T. Belloni, *Jets from black hole X-ray binaries: testing, refining and extending empirical models for the coupling to X-rays*, *MNRAS* **396** (2009) 1370.
- [7] J. Homan, et al., *A Rapid Change in X-Ray Variability and a Jet Ejection in the Black Hole Transient MAXI J1820+070*, *ApJL* **891** (2020) L29.